JCTC Journal of Chemical Theory and Computation

Influence of Nitroxide Spin Labels on RNA Structure: A Molecular Dynamics Simulation Study

Hang Yu,[†] Yuguang Mu,*[,†] Lars Nordenskiöld,[†] and Gerhard Stock*[,‡]

School of Biological Sciences, Nanyang Technological University, Singapore 637551, and Institute of Physical and Theoretical Chemistry, J. W. Goethe University, D-60438 Frankfurt, Germany

Received July 8, 2008

Abstract: Pulsed electron double resonance (PELDOR) experiments on oligonucleotides provide a distance ruler that allows the measurement of nanometer distances accurately. The technique requires attachment of nitroxide spin labels to the nucleotides, which may possibly perturb its conformation. To study to what extent nitroxide spin labels may affect RNA structure, all-atom molecular dynamics simulations in explicit solvent are performed for six double-labeled RNA duplexes. A new parametrization of the force field for the nitroxide spin label is developed, which leads to intramolecular distances that are in good agreement with experimental results. Comparison of the results for spin-labeled and unlabeled RNA reveals that the conformational effect of the spin label depends significantly on whether the spin label is attached to the major or the minor groove of RNA. While major-groove spin labeling may to some extent affect the conformation of nearby base pairs, minor-groove spin labeling has the advantage of mostly preserving the RNA conformation.

Introduction

Nucleic acid conformations have been extensively studied since the discovery of central dogma in biochemistry.[1,2] As one of the key molecules in biological processes, RNA has gained major interest in its structure and folding, especially after the discovery of gene regulation function in RNA interference.[3] Together with an increasing number of resolved structures, this may facilitate the use of RNA as a potential target in drug design.[4]

As crystallography may only partly represent the structures and dynamics in the cellular environment, alternative spectroscopic methods like electron paramagnetic resonance (EPR),[5] nuclear paramagnetic resonance (NMR),[6] and fluorescence resonance energy transfer (FRET)[7] can provide complementary information on structures in solution that resemble biological conditions. EPR spectroscopy has been an effective method for structural characterization of RNA.[8−10] In particular, pulsed electron double resonance (PELDOR) can measure intramolecular distances ranging from 14 to 50 Å with 1 Å precision.[11,12] To be detectable by EPR, labels such as nitroxide spin labels (see Figure 1) need to be attached to RNA.[13] Various approaches to spin labeling of nucleotides have been proposed.[8,12,14−16] Site-directed spin label attachment to the 2′-sugar position of nucleic acids have been found to lead to relatively broad distance distributions.[8] Using a flexible C—S linkage attached to backbone phosphorothioate allows easy and fast synthesis. A simulation study of spin-labeled DNA duplexes with a flexible C—S linkage demonstrated that such spin labels exert little perturbation to the structure of attached DNA,[16] but the flexible linkage might influence the result of nanometer ruler

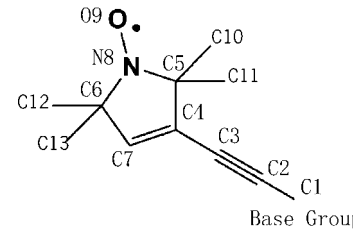

Figure 1. Structure and atom labeling of nitroxide spin label group.

* Corresponding author e-mail: ygmu@ntu.edu.sg (Y.M.) and stock@theochem.uni-frankfurt.de (G.S.).

[†] Nanyang Technological University.

[‡] J. W. Goethe University.

10.1021/ct800266e CCC: $40.75
Published on Web 09/09/2008

Table 1. Sequences of slRNA and cRNA[a]

RNA	sequence	RNA	sequence
1	5′GCUGAUA**U**CAGC	**4**	5′GCUGUAU**A**CAGC
	3′CGAC**U**AUAGUCG		3′CGAC**A**AUAUGUCG
2	5′GACUGAUCAG**U**C	**5**	5′CGUGUAUGCAUA**C**ACG
	3′C**U**GACUAGUCAG		3′GCA**C**AUACGUAUGUGC
3	5′CGACUGAUAUCAG**U**CG	**6**	5′CGCUACAUAG**U**GAGCG
	3′GC**U**GACUAUAGUCAGC		3′GCG**A**UGUAUCACUCGC

[a] Spin-labeled nucleotides are underlined. cRNA 1 and 4 are exactly the same sequence as spin-labeled RNA 1 and 4, respectively, but without spin label.

measurement.[15] Recently, a new labeling method via a rigid R−C≡C−C linkage at the nucleic acid base has been proposed, which facilitates accurate PELDOR measurements of distances between two labels in a range of 19−53 Å.[12,14] For example, distance measurements in various RNA duplexes have facilitated the discrimination of A- and B-form conformation.[14]However, it is not yet clear to what extent the rigid linker at the nucleic acid base will influence the structural and dynamical properties of the RNA attached.

To fully assess the potential of this spin labeling method and the associated PELDOR measurements, the conformational flexibility of the labels and their influence on RNA structure need to be investigated. To this end, we perform all-atom molecular dynamics (MD) simulations in explicit solvent for six double-labeled RNA duplexes. Due to improved nucleic acid force fields and appropriate description of the electrostatic, MD studies have emerged as a versatile tool to study the structure and dynamics of RNA systems in atomistic detail.[17−25] A new parametrization of force field for the nitroxide spin label is developed, which represents an improvement of our previous work.[12] We show that the new model leads to intramolecular RNA distances that are in good agreement with existing experimental results. Comparison of the results for spin-labeled and unlabeled RNA reveals that the conformational effect of the spin label depends significantly on whether the spin label is attached to the major or the minor groove of RNA. While major-groove spin labeling may affect the conformation of nearby base pairs, minor-groove spin labeling has the advantage of mostly preserving the RNA conformation.

Methods

1. RNA Systems. Following the experimental investigations,[14] we studied six duplex RNAs (RNA1 to RNA6) of various lengths and sequences, see Table 1. We considered two types of spin labels, which differ in their position relative to RNA. Spin labels attached at the C5 position of pyrimidine bases are located in the *major* groove of RNA. This concerns spin labels at uracil bases in spin-labeled (sl) RNA1−RNA3 and of cytosine bases in slRNA5. On the other hand, spin labels attached to purine bases at the C2 position are located in the *minor* groove of RNA. This is the case for the spin labels on adenine bases in slRNA4. Finally, we considered a mixed case, slRNA6, which contains a labeled adenine located in the minor groove and a labeled uracil in the major groove. To compare the behavior of labeled and unlabeled RNA, we also studied unlabeled control RNA1 and RNA4, referred to as cRNA1 and cRNA4.

2. Force Field. In all simulations, the GROMACS (version 3.3) software package[26] combined with the Amber98 force field[27] was used. For slRNA1 and slRNA4 an additional 50 ns simulations were performed, using the recent Amber parametrization parmbsc0[28] which avoids artificial transitions along the backbone torsion angles α and γ.[29,30] However, the average structural properties such as the A-form percentage obtained for both force fields were quite similar. This indicates that our general results concerning the perturbation of RNA conformation by spin labels does not depend on the nucleic acid force field.

The force field parameters for the nitroxide spin label (Figure 1) were obtained via Hartree−Fock (HF) calculations with 6−31G* basis set using Gaussian03 program.[31] Adopting AMBER force field parametrization philosophy,[32] all parameters of the bonded interactions of the spin label were generated, see Table 2. Partial charges were derived from the HF/6−31G* calculations and fitted with the RESP algorithm using the R.E.D program.[33] Standard AMBER force field parameters were assumed for the remaining nonbonded interactions. The resulting force field parameters for the nitroxide spin label represent an improvement over our previous simpler parametrization,[12] which assumed a rigid artificial long bond between C1 and C4 (Figure 1). When applied to reproduce the quantitative orientation and distance distribution of model biradicals,[34] the previous force field was found to behave too rigidly because of these simplifications. The new parameters are largely consistent with the parametrization recently published by Darian and Gannett.[35] However, two bond angles on the five-member ring, C5−C4−C7 and C4−C7−C6 (in their nomenclature C3−C4−C5 and C1−C5−C4), are different. Our values are 112.3° and 112.9° and their values are both 120°, resulting in a sum of the five ring bond angles of 539.9° (our model) and 553.82° (their model). So our model better describes the planar nature of the ring.

3. MD Simulation Details. All RNA systems considered (labeled slRNA1−slRNA6 as well as unlabeled cRNA1 and cRNA4) were solvated in a rectangular box of TIP3P water,[36] keeping a minimum distance of 10 Å between the solute and each face of the box. Sodium counterions were added to neutralize the system, and water molecules overlapping with ions were removed. The numbers of total atoms in the simulation box are 25151, 21557, 31937, 22236, 32823, 32237 for slRNA1−slRNA6, respectively. The equation of motion was integrated by using a leapfrog algorithm[37] with a time step of 2 fs. Covalent bond lengths involving hydrogen atoms were constrained by the procedure SHAKE[38] with a relative geometric tolerance of 0.0001. We used a particle-mesh Ewald treatment for the long-range electrostatics.[39] The pair list of nonbonded interaction was updated every 10 fs. The solute and solvent were separately weakly coupled to external temperature baths at 300 K.[40] The temperature coupling constant was 0.5 ps. The total system was weakly coupled to an external pressure bath at 1 atm using a coupling constant of 5 ps.

Starting from canonical A-form, all RNAs were minimized *in vacuo* for 1000 steps to relax the initial structural constrains. After minimization, the RNAs were solvated in

Table 2. Force Field Parameters for Spin Label

atoms	C1	C2	C3	C4	C5	C6	C7	N8	O9
charges(e)	−0.0710	−0.1787	−0.0443	−0.0202	0.2853	0.2312	−0.2147	0.1769	−0.4037
type	C2	CZ	CZ	CM	CT	CT	CM	NA	O
atoms	HC7	C10	H1C10	C11	H1C11	C12	H1C12	C13	H1C13
charges(e)	0.1702	−0.2023	0.0592	−0.2023	0.0592	−0.2948	0.0876	−0.2948	0.0876
type	H5	CT	HT	CT	HT	CT	HT	CT	HT
bonds	C1−C2	C2−C3	C3−C4	C4−C5	C5−N8	N8−O9	C6−N8	C6−C7	C4−C7
l_{bond} (nm)	0.144	0.12	0.144	0.15	0.146	0.125	0.146	0.15	0.1318
k_{bond}(kJ/nm^2)	251040	292880	251040	265265	355682	241000	355681	224262	265265
bonds	C5−C10	C5−C11	C6−C12	C6−C13	C10−H1C10				
l_{bond} (nm)	0.153	0.153	0.153	0.153	0.108				
k_{bond}(kJ/nm^2)	251040	251040	251040	251040	307106				

angles	C1−C2−C3	C2−C3−C4	C3−C4−C5	C3−C4−C7	C4−C5−N8	C5−N8−O9	C5−N8−C6	C6−N8−O9	N8−C6−C7	C6−C7−C4
A_0(degree)	180	180	120	120	99.4	122.1	115.7	122.2	99.6	112.9
K_{angle}(kJ/mol rad^2)	556	556	644	644	544	503	563	503	527	527
angles	N8−C5−C10	C10−C5−C11	C6−C7−HC7	C4−C7−HC7	C7−C4−C5					
A_0(degree)	110.4	110.7	122.1	125.0	112.3					
K_{angle}(kJ/mol rad^2)	560	560	780	790	545					

Table 3. Molecular Dynamics Characterization of Spin-Labeled RNAs

slRNA	1	2	3	4	5	6
$<d_{SL}>_{PELDOR}$ [Å]	19.3 ± 1.2	33.7 ± 3.9	38.7 ± 1.3	21.9 ± 0.8	33.6 ± 1.6	26.9 ± 1.3
$<d_{SL}>_{MD}$ [Å]	17.2 ± 1.8	31.3 ± 1.8	36.4 ± 2.2	22.8 ± 0.7	34.3 ± 1.8	24.6 ± 2.4
$<d_B>$ [Å]	10.8 ± 0.6	28.1 ± 1.3	32.3 ± 1.7	12.4 ± 0.5	28.3 ± 0.9	23.4 ± 1.2
correlation	0.6	0.6	0.5	0.6	0.7	0.7
rmsd [Å]	2.8	1.9	2.6	2.6	2.6	3.4
A-form [%]	78.1	60.1	58.1	73.0	75.3	80.9
populations[%]	55/24/8	59/14/11	77/7/6	97/1/1	89/5/2	70/10/7

Listed are the internitroxide distances of the spin labels obtained from PELDOR experiments ($<d_{SL}>_{PELDOR}$)[14] and MD calculations ($<d_{SL}>_{MD}$) and the corresponding interbase distances $<d_B>$, the correlation coefficient between $<d_{SL}>_{MD}$) and $<d_B>$, the mean RMSD with respect to ideal A-form, the percentage of A-form conformation, the number of clusters, and the population probability of the two most populated clusters.

TIP3P water, and a 100 ps simulation of water molecules and counterions was performed with fixed solute, followed by a 100 ps NPT run without constraining the solute. Subsequently, the simulation was continued for 50 ns at constant temperature (300 K) and pressure (1 atm), whereby the coordinates were saved every 0.1 ps for analysis.

4. Analysis of Trajectories. Root mean squared deviations (rmsd) of all RNAs were calculated with respect to initially perfect A-form configuration. Internitroxide distances were measured as the distance between the nitrogen atoms of the two spin labels. Interbase distances were measured as the distance between carbon atoms of the base to which the spin labels were attached (C5 on purine, C2 on pyrimidine). The A-form of RNA is characterized by the quantity *Zp*, representing the mean *z*-coordinate of the backbone phosphorus atoms (with respect to individual dimer reference frames) that are greater than 1.5 Å for A-type and less than 0.5 Å for B-form steps.[41] Major and minor groove widths were defined from the distance between two phosphate atoms on the RNA backbone, with phosphate atom radius included.[41] Helical parameters as well as base pair conformations (classified as A, B, and TA-form) were calculated using the programs X3DNA[42] and CURVES 5.0.[43] Structural snapshots were selected every 5 ps for clustering. The clustering algorithm[44] was based on pairwise RMSDs with a cutoff of 2 Å for all atoms. The structural snapshot at the center of each cluster was taken as its representative structure.

Results and Discussion

1. Intramolecular Distances. Distance calculations from previous MD simulations of RNA using an earlier version of the spin label force field were in good agreement with experimental PELDOR distances.[14] To get a first impression on the quality of the new force field, we therefore again compare calculated and experimental internitroxide distances for all spin-labeled RNAs. As shown in Table 3, we find good overall agreement of theory and experiment, with somewhat better results for slRNAs 2, 3, and 4 than obtained by the previously used model. Although the main reason for the reparameterization of the spin label force field was a better description of the spin label dynamics,[34] it is nevertheless reassuring that the new force field also yields a somewhat improved description of the overall structure.

For the interpretation of PELDOR experiments, it is interesting to know to what extent the internitroxide distances of the spin labels monitor the corresponding interbase distances in the RNA (see Methods for definitions). Figure 2 shows the time evolution of both quantities for all spin-labeled RNAs. As a consequence of the relative orientation of the two spin labels, the absolute values of internitroxide

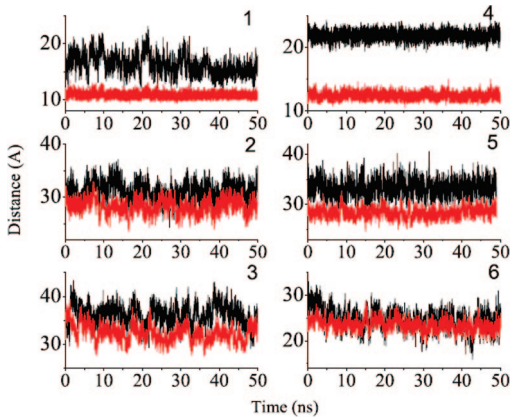

Figure 2. Time evolution of the internitroxide (black) and interbase (red) distances of slRNA1−slRNA6.

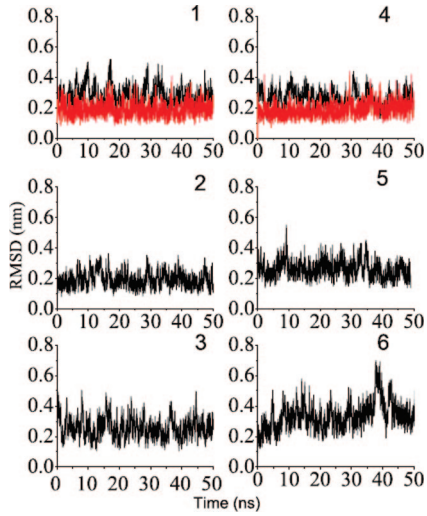

Figure 3. Time evolution of the rmsd of spin-labeled slRNA1−slRNA6 (black) and unlabeled cRNA1 and cRNA4 (red).

and interbase distances may differ significantly. In particular, that is the case for slRNA4 which has the spin labels located in the minor groove.

For all systems, the patterns of the time traces are quite similar for internitroxide and interbase distances. As listed in Table 3, we typically find a correlation coefficient of ≈0.6. The similar pattern indicates that the motions of the spin labels are mainly due to the motion of RNA bases instead of the flexibility of the spin labels. Compared to the spin-labeling method using a flexible C—S linkage,[15,16] the rigidity of the spin labels in the present approach allows for a more direct observation of the base pair movement and therefore a more accurate and sensitive probing of RNA conformation.

2. Structure of Spin-Labeled RNA. A well-known measure for the overall stability of a MD simulation is the rmsd along a trajectory (see Methods for definition). Figure 3 shows the time evolution of the rmsd (with respect to ideal A-form) of all labeled and unlabeled RNAs considered. With the exception of slRNA1 and slRNA6, the RMSDs of the spin-labeled RNAs fluctuate steadily around 2−3 Å (see Table 3 for mean RMSDs). It is interesting to compare the RMSDs of slRNA1 (as an example for major-groove

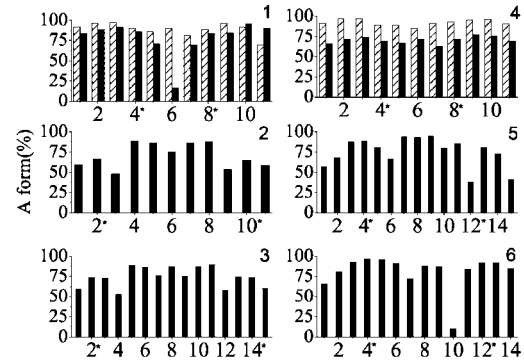

Figure 4. Percentage of time in which base pair steps maintain A-form conformation. Shown are spin-labeled slRNA1−slRNA6 (black columns) and unlabeled cRNA1 and cRNA4 (shaded columns). The base pair step which contains the spin-labeled base is marked by an asterisk.

labeling) and slRNA4 (as an example for minor-groove labeling) to the RMSDs of the corresponding unlabeled cRNA1 and cRNA4. In both cases we find a significant increase of the RMSDs upon labeling. This finding is in agreement with the observation that spin-labeled RNAs exhibit lower melting temperatures than unlabeled RNAs.[14]

The significant structure in the rmsd time traces of slRNA1 and slRNA6 can be explained as conformational transitions of these systems. In fact, a clustering of the RNA structures of all trajectories reveals that only the minor-groove labeled slRNA4 remains essentially (>96%) in a single conformation, see Table 3. This is similar to the two unlabeled cRNA1 and cRNA4, which are found to occur in two clusters of 97% and 3% population, respectively. On the other hand, the major-groove labeled slRNAs show several thermally populated conformational states. This observation is in line with PELDOR measurements that show an increased damping of the PELDOR time traces for major-groove labeled slRNAs.[14]

As an alternative measure of the stability of RNA structure, we next consider the RNA base pair conformation, which can be roughly classified into A-form, B-form, and other structures (see Methods for definitions). To this end, Figure 4 shows the mean percentage of the A-form structure of all spin-labeled RNAs. Most of the base steps are found to maintain A-form conformation and intact base pairing for over 70% of time during simulation. Exceptions are again slRNA1 and slRNA6, which both show that one base step *between* the spin labels exhibits significantly low A-form content. Comparison with unlabeled cRNA1 and cRNA4 shows that spin labeling appears to somewhat reduce the A-form probability.

3. Effects of Major-Groove Spin Labeling. The results presented above have shown that the structural and dynamical effects of spin labeling in the major-groove are most prominent in slRNA1. In the following, we therefore adopt this system for further analysis. Although the spin labels of this RNA are attached at base steps 5 and 8, Figure 4 shows that mainly the structure of base step 6 deviates from A-form. This suggests that spin label in the major groove somehow deforms the conformation of the neighboring base pairs.

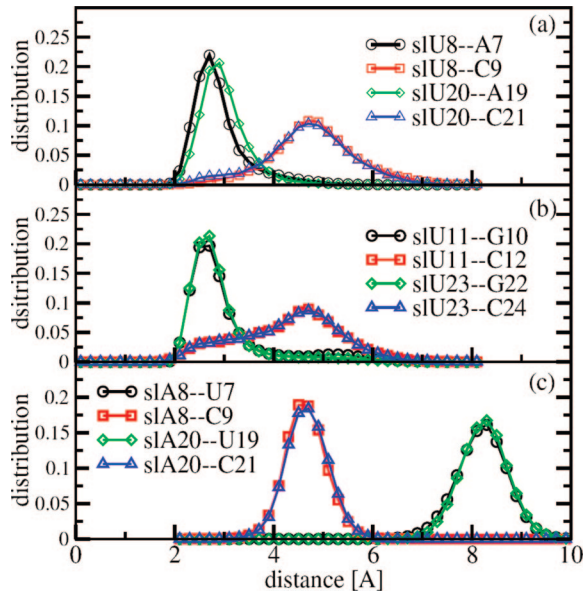

Figure 5. MD distribution of minimum distances between the two spin-label groups and their neighbor base in slRNA1 (a), slRNA2 (b), and slRNA4 (c).

The steric influence of the spin label groups can be estimated by calculating the minimum distance between the atoms of the spin label (C4−C13 in Figure 1) and the neighboring base atoms of the same strand. As an example, Figure 5(a) displays the distribution of the minimum distances between the spin label group on U8 and neighbor bases A7 and C9 as well as between the spin label group on U20 and neighbor bases A19 and C21. In the case of A-U_{SL}, where the distance is measured between the base of adenine and the spin label of uracil, we obtain a mean distance of ≈2.4 Å in both cases. That is, for more than 73% of the simulation time the uracil spin labels are in close contact (≤2.5 Å) with the adenine bases. Such close contacts perturb the base configuration and may cause the opening of base pairs U6-A19 and A7-U18,[14] thus resulting in a low A-form content. The situation is similar in the case of G-U_{SL} contacts found in slRNA2 (see Figure 5(b)) and slRNA3, which also show a mean distance of ≈2.4 Å in all cases considered. Further evidence of the effect of the spin label is gained by considering the width of the major groove. Comparing, e.g., spin-labeled slRNA1 and unlabeled cRNA1, Figure 6 shows that the label widens the major groove around the spin-labeled residues.

We note that base pairs U6-A19 and A7-U18 are the nearest neighbors to the spin-labeled bases in the 3′ direction. In contrast, the two base pairs G4-C21 and C9-G16 are the nearest neighbors in the 5′ direction. These base pairs exhibit a mean distance of ≈4.5 Å to the spin labels and are therefore rarely in close contact with the spin labels. In summary, due to the narrow and deep nature of the RNA major groove, we find close contacts (≤2.5 Å) of uracil spin labels with nearest neighboring bases in the 3′ direction, while we find sufficient space (≈4.5 Å) of uracil spin labels with nearest-neighbor bases in the 5′ direction. This finding is nicely illustrated in Figure 6, which shows representative MD snapshots of spin-labeled slRNA1 (a) and unlabeled cRNA1 (b).

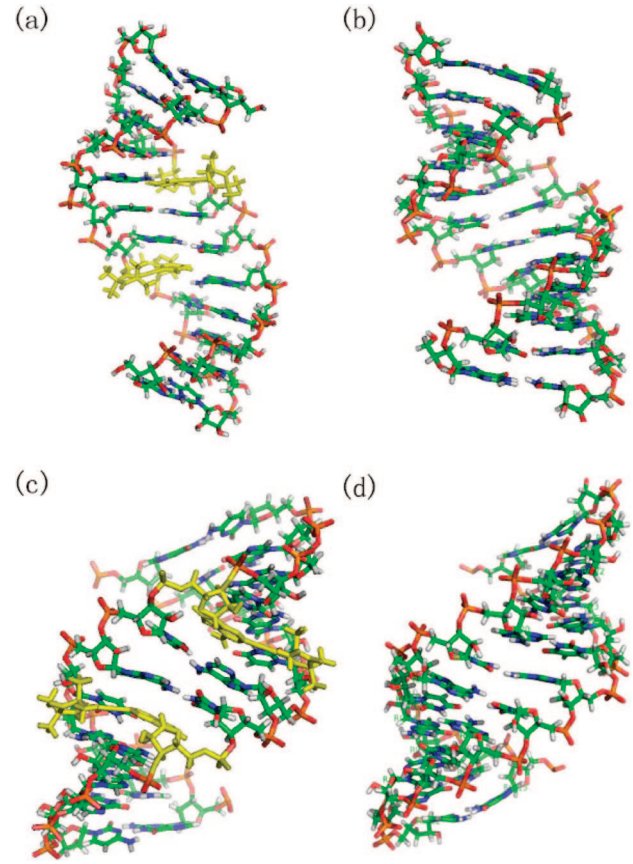

Figure 6. Representative MD snapshots of spin-labeled slRNA1(a) and slRNA4(c) as well as of the corresponding unlabeled cRNA1 (b) and cRNA4 (d). Structures are viewed from a major groove in (a) and (b) and from a minor groove in (c) and (d). Spin-labeled residues are colored in yellow.

4. Effect of Minor-Groove Spin Labeling. The comparison of the computational results for minor groove spin-labeled slRNA4 with the results for the corresponding unlabeled cRNA4 reveals that the spin label hardly influences the structures of the RNA. Although the overall rmsd is somewhat increased (Figure 3) and the A-form content is somewhat decreased (Figure 4) upon labeling, there is no indication for local distortion of RNA as it is the case for major groove spin-labeled slRNA1 (Figure 7). Moreover, slRNA4 is found 97% of the time in a single conformational state (Table 3). These findings are in line with the distribution of the distances between the two spin label head groups and base pairs 6 and 7 (Figure 5(c)), which reveals that there is no close contact (≤2.5 Å) between spin labels and neighboring base pairs. Furthermore, Figure 6 shows that the groove widths of the labeled slRNA4 do not change evidently compared with the unlabeled cRNA4.

Conclusions

We have developed a new parametrization of the force field for the nitroxide spin label, which was shown to lead to intramolecular distances that are in good agreement with experimental results. Employing this force field, we have studied in detail the effects of the labels on various RNA duplex structures. Nitroxide spin labels attached to pyrimidine bases such as uracil and cytosine at the C5 position are

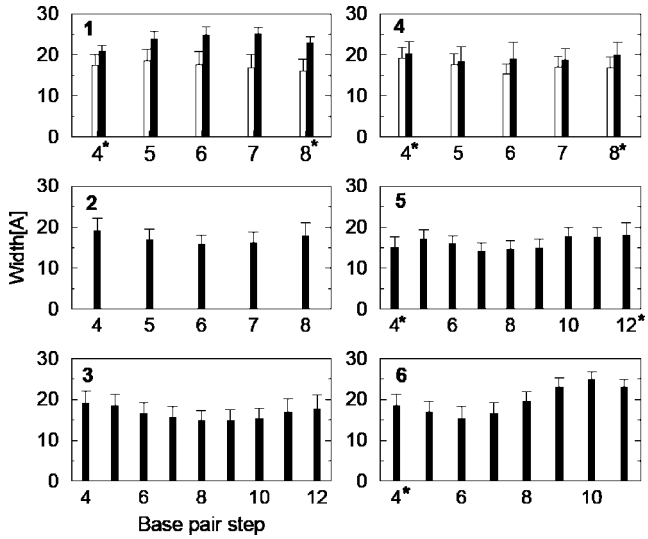

Figure 7. Average major groove width of spin-labeled RNA1−6 (black columns) and unlabeled cRNA1 and cRNA4 (white columns). The base pair step which contains the spin-labeled base is marked by an asterisk.

located in the major groove, while labels attached to purine bases such as adenine at the C2 position are located in the minor groove. While there is ample space for the label in the minor groove, spin labeling in the major groove may lead to close contacts of the label and the neighbor bases, particularly in the 3′ direction. Such close contacts perturb the base configuration and may cause the opening of the neighbor base pairs, thus resulting in a low A-form content.

Interestingly, the situation is different for spin labeling of DNA duplexes,[35] where the label mostly affected the conformation of the labeled base pair rather than the adjacent base pairs. This is caused by the different structures of DNA and RNA duplexes: While RNA mainly adopts the B-form conformation, RNA is mainly found as an A-form helix which forms a deep and narrow major groove. Hence the A-form base pairs force the rigid spin label to incline in the 3′ direction, thus getting into close contact with base pairs that are one step down to the spin-labeled bases.

Acknowledgment. We thank T. F. Prisner, O. Schiemann, and J. W. Engels for numerous inspiring and helpful discussions and a long-standing collaboration. Furthermore, Y.M. gratefully acknowledges support from the University Research Committee (URC, RG65/06 grant) and the Ministry of Education AcRF Tier 2 grant (T206B3210RS), L.N. gratefully acknowledges support from the Ministry of Education AcRF Tier 2 grant (T206B3207), and G.S. gratefully acknowledges support from the Deutsche Forschungsgemeinschaft (via SFB 579 RNA-ligand interactions), the Fonds der Chemischen Industrie, and the Frankfurt Center for Scientific Computing.

References

(1) Crick, F. H. C. *What Mad Pursuit*; Basic Books: New York, 1988.

(2) Judson, H. F. *The Eighth Day of Creation*; Simon & Schuster: New York, 1980.

(3) Denli, A. M.; Hannon, G. J. RNAi: an ever-growing puzzle. *Trends Biochem. Sci.* **2003**, *28*, 196.

(4) Delihas, N.; Rokita, S. E.; Zheng, P. Natural antisense RNA/target RNA interactions: Possible models for antisense oligonucleotide drug design. *Nat. Biotechnol.* **1997**, *15*, 751.

(5) Eaton, S. S. *Biomedical EPR*; Kluwer Academic/Plenum Publishers: New York, 2005.

(6) Vliegenthart, J. F. G. *NMR spectroscopy and computer modeling of carbohydrates: recent advances*; American Chemical Society: New York, 2006.

(7) Periasamy, A. *Molecular imaging: FRET microscopy and spectroscopy*; Published for the American Physiological Society by Oxford University Press: New York, 2005.

(8) Schiemann, O.; Fritscher, J.; Kisseleva, N.; Sigurdsson, S. T.; Prisner, T. F. Structural investigation of a high-affinity MnII binding site in the hammerhead ribozyme by EPR spectroscopy and DFT calculations. Effects of neomycin B on metal-ion binding. *Chembiochem* **2003**, *4*, 1057.

(9) Horton, T. E.; DeRose, V. J. Cobalt hexammine inhibition of the hammerhead ribozyme. *Biochemistry* **2000**, *39*, 11408.

(10) Qin, P. Z.; Dieckmann, T. Application of NMR and EPR methods to the study of RNA. *Curr. Opin. Struct. Biol.* **2004**, *14*, 350.

(11) Jeschke, G. Distance measurements in the nanometer range by pulse EPR. *Chemphyschem* **2002**, *3*, 927.

(12) Schiemann, O.; Piton, N.; Mu, Y.; Stock, G.; Engels, J. W.; Prisner, T. F. A PELDOR-based nanometer distance ruler for oligonucleotides. *J. Am. Chem. Soc.* **2004**, *126*, 5722.

(13) Werner, H. J.; Schulten, K.; Weller, A. Electron transfer and spin exchange contributing to the magnetic field dependence of the primary photochemical reaction of bacterial photosynthesis. *Biochim. Biophys. Acta* **1978**, *502*, 255.

(14) Piton, N.; Mu, Y.; Stock, G.; Prisner, T. F.; Schiemann, O.; Engels, J. W. Base-specific spin-labeling of RNA for structure determination. *Nucleic Acids Res.* **2007**, *35*, 3128.

(15) Cai, Q.; Kusnetzow, A. K.; Hideg, K.; Price, E. A.; Haworth, I. S.; Qin, P. Z. Nanometer distance measurements in RNA using site-directed spin labeling. *Biophys. J.* **2007**, *93*, 2110.

(16) Price, E. A.; Sutch, B. T.; Cai, Q.; Qin, P. Z.; Haworth, I. S. Computation of nitroxide-nitroxide distances in spin-labeled DNA duplexes. *Biopolymers* **2007**, *87*, 40.

(17) Cheatham, T. E., III. Simulation and modeling of nucleic acid structure, dynamics and interactions. *Curr. Opin. Struct. Biol.* **2004**, *14*, 360.

(18) Sanbonmatsu, K. Y.; Joseph, S.; Tung, C.-S. Simulating movement of tRNA into the ribosome during decoding. *Proc. Natl. Acad. Sci. U.S.A.* **2005**, *102*, 15854.

(19) Auffinger, P.; Westhof, E. RNA hydration: three nanoseconds of multiple molecular dynamics simulations of the solvated tRNAAsp anticodon hairpin. *J. Mol. Biol.* **1997**, *269*, 326.

(20) Pan, Y.; Priyakumar, U. D.; MacKerell, A. D. Conformational Determinants of Tandem GU Mismatches in RNA: Insights from Molecular Dynamics Simulations and Quantum Mechanical Calculations. *Biochemistry* **2005**, *44*, 1433.

(21) Mu, Y. G.; Stock, G. Conformational dynamics of RNA-peptide binding; A molecular dynamics simulation study. *Biophys. J.* **2006**, *90*, 391.

(22) Koplin, J.; Mu, Y. G.; Richter, C.; Schwalbe, H.; Stock, G. Structure and dynamics of an RNA tetraloop: A joint

molecular dynamics and NMR study. *Structure* **2005**, *13*, 1255.

(23) Clerte, C.; Hall, K. B. Characterization of multimeric complexes formed by the human PTB1 protein on RNA. *RNA* **2006**, *12*, 457.

(24) Sorin, E. J.; Engelhardt, M. A.; Herschlag, D.; Pande, V. S. RNA simulations: probing hairpin unfolding and the dynamics of a GNRA tetraloop. *J. Mol. Biol.* **2002**, *317*, 493.

(25) Barthel, A.; Zacharias, M. Conformational transitions in RNA single uridine and adenosine bulge structures: A molecular dynamics free energy simulation study. *Biophys. J.* **2006**, *90*, 2450.

(26) Van Der Spoel, D.; Lindahl, E.; Hess, B.; Groenhof, G.; Mark, A. E.; Berendsen, H. J. GROMACS: fast, flexible, and free. *J. Comput. Chem.* **2005**, *26*, 1701.

(27) Cheatham, T. E., III.; Cieplak, P.; Kollman, P. A. A modified version of the Cornell et al. force field with improved sugar pucker phases and helical repeat. *J. Biomol. Struct. Dyn.* **1999**, *16*, 845.

(28) Perez, A.; Marchan, I.; Svozil, D.; Sponer, J.; Cheatham, T. E.; Laughton, C. A.; Orozco, M. Refinement of the AMBER force field for nucleic acids: improving the description of alpha/gamma conformers. *Biophys. J.* **2007**, *92*, 3817.

(29) Beveridge, D. L.; Barreiro, G.; Byun, K. S.; Case, D. A.; Cheatham, T. E., III.; Dixit, S. B.; Giudice, E.; Lankas, F.; Lavery, R.; Maddocks, J. H.; Osman, R.; Seibert, E.; Sklenar, H.; Stoll, G.; Thayer, K. M.; Varnai, P.; Young, M. A. Molecular dynamics simulations of the 136 unique tetranucleotide sequences of DNA oligonucleotides. I. Research design and results on d(CpG) steps. *Biophys. J.* **2004**, *87*, 3799.

(30) Varnai, P.; Zakrzewska, K. DNA and its counterions: a molecular dynamics study. *Nucleic Acids Res.* **2004**, *32*, 4269.

(31) Frisch, M. J. T. G. W.; Schlegel, H. B.; Scuseria, G. E.; Robb, M. A.; Cheeseman, J. R.; Montgomery, J. A., Jr.; Vreven, T.; Kudin, K. N.; Burant, J. C.; Millam, J. M.; Iyengar, S. S.; Tomasi, J.; Barone, V.; Mennucci, B.; Cossi, M.; Scalmani, G.; Rega, N.; Petersson, G. A.; Nakatsuji, H.; Hada, M.; Ehara, M.; Toyota, K.; Fukuda, R.; Hasegawa, J.; Ishida, M.; Nakajima, T.; Honda, Y.; Kitao, O.; Nakai, H.; Klene, M.; Li, X.; Knox, J. E.; Hratchian, H. P.; Cross, J. B.; Bakken, V.; Adamo, C.; Jaramillo, J.; Gomperts, R.; Stratmann, R. E.; Yazyev, O.; Austin, A. J.; Cammi, R.; Pomelli, C.; Ochterski, J. W.; Ayala, P. Y.; Morokuma, K.; Voth, G. A.; Salvador, P.; Dannenberg, J. J.; Zakrzewski, V. G.; Dapprich, S.; Daniels, A. D.; Strain, M. C.; Farkas, O.; Malick, D. K.; Rabuck, A. D.; Raghavachari, K.; Foresman, J. B.; Ortiz, J. V.; Cui, Q.; Baboul, A. G.; Clifford, S.; Cioslowski, J.; Stefanov, B. B.; Liu, G.; Liashenko, A.; Piskorz, P.; Komaromi, I.; Martin, R. L.; Fox, D. J.; Keith, T.; Al-Laham, M. A.; Peng, C. Y.; Nanayakkara, A.; Challacombe, M.; Gill, P. M. W.; Johnson, B.; Chen, W.; Wong, M. W.; Gonzalez, C.; Pople, J. A. *Gaussian 03, Revision C.02*; Gaussian: Wallingford, CT, 2004.

(32) Case, D. A.; Pearlman, D. A.; Caldwell, J. C.; Cheatham, T. E., III.; Ross, W. S.; Simmerling, C. L.; Darden, T. A.; Merz, K. M.; Stanton, R. V.; Cheng, A. L.; Vincent, J. J.; Crowley, M.; Tsui, V.; Radmer, R. J.; Duan, Y.; Pitera, J.; Massova, I.; Sibel, G. L.; Singh, U. C.; Weiner, P. K.; Kollman, P. A. *AMBER 6*; University of California: SF, 1999.

(33) Pigache, A.; Cieplak, P.; Dupradeau, F. Y. Automatic and highly reproducible RESP and ESP charge derivation: Application to the development of programs RED and X RED. In *227th ACS National Meeting,* Anaheim, CA, 2004.

(34) Marko, A.; Margraf, D.; Mu, Y.; Stock, G.; Prisner, T. ; Quantification of oreintation selection in PELDOR experiments. Manuscript in preparation for J. Chem. Phys. **2008**.

(35) Darian, E.; Gannett, P. M. Application of molecular dynamics simulations to spin-labeled oligonucleotides. *J. Biomol. Struct. Dyn.* **2005**, *22*, 579.

(36) Jorgensen, W. L.; Chandrasekhar, J.; Madura, J. D.; Impey, R. W.; Klein, M. L. K. Comparison of simple potential functions for simulating liquid water. *J. Chem. Phys.* **1983**, *79*, 926.

(37) Verlet, L. Computer "Experiments" on Classical Fluids. I. Thermodynamical Properties of Lennard-Jones Molecules. *Phys. Rev.* **1967**, *159*, 98.

(38) Ryckaert, J.-P.; Ciccotti, G.; Berendsen, H. J. C. Numerical integration of the cartesian equations of motion of a system with constraints: molecular dynamics of n-alkanes. *J. Comput. Phys.* **1977**, *23*, 327.

(39) Tom, D.; Darrin, Y.; Lee, P. Particle mesh Ewald: An N log(N) method for Ewald sums in large systems. *J. Chem. Phys.* **1993**, *98*, 10089.

(40) Berendsen, H. J. C.; Postma, J. P. M.; van Gunsteren, W. F.; Dinola, A.; Haak, J. R. Molecular-Dynamics with Coupling to an External Bath. *J. Chem. Phys.* **1984**, *81*, 3684.

(41) El Hassan, M. A.; Calladine, C. R. Two distinct modes of protein-induced bending in DNA. *J. Mol. Biol.* **1998**, *282*, 331.

(42) Lu, X.-J.; Olson, W. K. 3DNA: a software package for the analysis, rebuilding and visualization of three-dimensional nucleic acid structures. *Nucleic Acids Res.* **2003**, *31*, 5108.

(43) Lavery, R.; Sklenar, H. The definition of generalized helicoidal parameters and of axis curvature for irregular nucleic acids. *J. Biomol. Struct. Dyn.* **1988**, *6*, 63.

(44) Daura, X.; Gademann, K.; Jaun, B.; Seebach, D.; van Gunsteren, W. F.; Mark, A. E. Peptide folding: When simulation meets experiment. *Angew. Chem., Int. Ed.* **1999**, *38*, 236.

CT800266E